Structure sensitivity in the hydrodechlorination of chlorobenzene over supported nickel

Mark A. Keane *, Colin Park †, and Claudia Menini

Department of Chemical and Materials Engineering, University of Kentucky, Lexington, KY 40506-0046, USA

Received 3 December 2002; accepted 17 March 2003

The gas phase hydrodechlorination (HDC) of chlorobenzene (at 523 K) was studied over Ni/SiO_2 (prepared by precipitation–deposition and impregnation) and Ni-impregnated Al_2O_3, MgO, activated carbon and graphite; the Ni loading spanned the range 1.5–20.3% w/w. The activated catalysts (with and without precalcination) were characterized by TEM/H_2 chemisorption and the Ni particle size (distribution) is related to HDC activity. The levels of reversibly and irreversibly held Cl on the used catalysts were recorded: spent Ni/MgO bore the highest residual Cl. The reaction is structure sensitive, with an increase in specific HDC rate at higher (average) Ni particle sizes over the range 1.4–22.1 nm. The exception to this trend is Ni/graphite and (to a lesser extent) Ni/Al_2O_3, where Ni–support interactions are responsible for lowering the HDC activity.

KEY WORDS: chlorobenzene; hydrodechlorination; supported nickel; structure sensitivity.

1. Introduction

Chlorinated aromatic compounds are an established source of environmental pollution [1] and the presence of these non-biodegradable compounds in effluent discharges is of increasing concern owing to the mounting evidence of adverse ecological and public health impacts [2]. It is now accepted that a progressive approach to waste management must embrace reduction, re-use, recycling and (energy) recovery [3]. The application of catalytic hydrodechlorination (HDC) to the treatment of chlorinated waste fits well within this environmental remediation ethos, whereby the hazardous material is transformed into recyclable products in a closed system with no (or limited) toxic emissions. Such a strategy fosters sustainable development and is far more progressive than existing destructive (typically incineration) methodologies. In any case, chloroarenes fall into the category of Principal Organic Hazardous Constituents, compounds that are inherently difficult to combust ($T > 1700$ K) where the formation of hazardous dioxins and furans can result from incomplete incineration [4]. Gas-phase catalytic HDC is non-destructive with no directly associated NO_x/SO_x emissions, and is operable in a closed system with no thermally induced free radical reactions that can lead to toxic intermediates. Moreover, HDC can be employed as a pre-treatment step to detoxify concentrated chlorinated streams prior to biodegradation.

Chlorobenzene has been the most widely adopted model haloarene reactant to assess gas-phase catalytic HDC activity over Pd [5–8], Pt [9], Rh [6,7] and Ni [10–19] catalysts. The mechanism of C–Cl bond hydrogenolysis is still unresolved and an unambiguous link between catalyst structure and dechlorination rate has yet to emerge. Juszczyk *et al.* [20] noted a higher turnover frequency of both CF_3CFCl_2 and CCl_2F_2 for larger Pd particles supported on Al_2O_3 and attributed this to an ensemble effect. Armendia and co-workers [21,22] also found that the liquid-phase hydrodehalogenation of chlorobenzene and bromobenzene over Pd/SiO_2–$AlPO_4$ was enhanced at lower Pd dispersions. Catalyst deactivation is a feature of HDC over Pt and Pd systems [21,23,24], but larger metal particles appear to be more resistant to poisoning [22,24]. Catalyst deactivation has been attributed to metal sintering [25], coke deposition [9] and the formation of an unreactive surface metal halide [14,25]. We have shown previously [10–12,26] that nano-dispersed Ni on silica is highly effective in gas-phase chloroarene dechlorination with no significant short-term loss of catalytic activity. In this paper, we consider the possible role that Ni–support interaction(s) can play in the HDC of chlorobenzene (CB) by examining the action of a common (9 ± 1% w/w) Ni loading on SiO_2, Al_2O_3, MgO, graphite and activated carbon (AC). Moreover, the effect of Ni loading (1–20% w/w) on SiO_2 is also considered, employing impregnation and precipitation–deposition as catalyst synthesis routes.

2. Experimental

2.1. Catalyst preparation, activation and characterization

The SiO_2 (fumed), Al_2O_3 and MgO substrates were supplied by Sigma-Aldrich and used as received. Activated

* To whom correspondence should be addressed.
E-mail: makeane@engr.uky.edu
† Present address: Synetix, P.O. Box 1, Belasis Avenue, Billingham, Cleveland TS23 1LB, UK.

1011-372X/03/0500-0089/0

carbon (G-60, 100 mesh) was obtained from NORIT (UK) and graphite (synthetic 1–2 μm powder) from Sigma-Aldrich. Both carbonaceous materials underwent a demineralization (continuous agitation in 1 M HNO_3 for 7 days) to remove any residual metal impurities that could contribute to the catalytic step; they were then thoroughly washed with deionized water until the pH approached 7. A $9 \pm 1\%$ w/w Ni loading on each support was achieved by impregnation where an $Ni(NO_3)_2$ solution in 2-butanol was added dropwise at 353 K to the substrate with constant agitation (500 rpm). A lower loaded (4.5% w/w) Ni/SiO_2 was prepared by varying the $Ni(NO_3)_2$ solution concentration and a wider range of Ni loadings (1.5–20.3% w/w) was generated by employing the homogeneous precipitation–deposition preparative technique that has been described in detail elsewhere [27]. In the latter case, precipitation was carried out at 361 ± 1 K for 6 h under constant agitation at 600 rpm with a preadjusted pH of 2.8 and $Ni(NO_3)_2/H_2NCONH_2$ molar ratio of 0.4. The Ni content was determined (to within $\pm 2\%$) by atomic absorption spectrometry (Varian-Spectra AA-10); the samples were digested in 37% HF overnight at ambient temperature. Chemical analysis of the activated catalysts before and after use did not reveal any significant loss of Ni from the used samples. The catalyst precursors were dried overnight in air at 383 K and reduced by heating (10 K/min) to 673 K (maintained for 16 h) in 60 cm^3/min dry H_2. Selected catalysts underwent a precalcination (10 K/min in 60 cm^3/min dry air to 623 K) prior to reduction. Samples (before and after catalysis) for off-line TEM analysis (Philips CM200 FEGTEM microscope operated at an accelerating voltage of 200 keV) were cooled (in He) and passivated in a 2% v/v O_2–He mixture at room temperature. Specimens for analysis were prepared by ultrasonic dispersion in 2-butanol, evaporating a drop of the resultant suspension on to a holey carbon support grid; Ni particle size distribution profiles presented in this study are based on a measurement of over 400 individual particles. Selected area electron diffraction (SAED) confirmed that the Ni distributed over each support was present in the metallic form and not as an oxide. A secondary ion mass spectrometric analysis (VG ESCALAB) of the activated catalysts (pressed into indium foil) revealed only the presence of nickel and support; there was no evidence of even trace amounts of impurities (or potential promoters) on the surface. Nickel dispersion was also measured by pulse H_2 chemisorption, employing a commercial Quantachrome ChemBET 3000 unit; dispersion values were reproducible to better than $\pm 5\%$. Nitrogen BET surface area measurements were conducted at 77 K (Micromeritics TriStar) for each activated catalyst.

2.2. Catalytic procedure

All the catalytic reactions were carried out under atmospheric pressure, *in situ*, immediately after activation, in a fixed-bed glass reactor at 523 K. The catalytic reactor has been described previously in detail [10–12] but features pertinent to this study are given below. A microprocessor-controlled infusion pump (kd Scientific) was used to deliver the chlorobenzene (CB) feed via a glass–PTFE air-tight syringe and PTFE line and the vapor was carried through the catalyst bed in a stream of dry H_2. The catalytic measurements were made at W/F (catalyst weight/CB molar flow-rate) = 17–52 g/mol/h. The reactor was operated in the differential mode with fractional conversion of the inlet CB feed <0.10; the overall gas space velocity was 2250 h^{-1}. The catalytic system has been shown [11] to operate with negligible diffusion constraints (effectiveness factor $(\eta) > 0.99$ at 573 K). Heat transport effects can also be disregarded; the temperature differential between the catalyst particles and bulk fluid phase was <1 K. The reactor effluent was analyzed by capillary GC as described elsewhere [10]; the reaction was monitored for <100 min on-stream, which was sufficient in each case to achieve a steady-state conversion. A chlorine (in the form of HCl product) mass balance was performed by passing the effluent gas through an aqueous NaOH ($(3–8) \times 10^{-3}$ mol/dm agitated at ≥ 300 rpm) trap with pH and potentiometric analyzes (Metrohm Model 728 Autotitrator) of the scrubbing solution [11]; the Cl mass balance was complete to better than $\pm 10\%$. In a separate set of experiments, the residual "reversibly" and "irreversibly" held Cl components on the catalyst after use were determined. The "reversibly" held Cl was desorbed from the catalyst after reaction by TPD (10 K/min to 723 K) with an isothermal hold at the final temperature for 16 h. The effluent stream was trapped in the NaOH scrubbing solution and the Cl content determined as above. The "irreversibly" held halogen content was then measured by heating a known weight (ca. 0.2 g) of the spent catalyst after TPD under reflux in deionized water for 24 h with the same potentiometric analysis. The thermal desorption treatment in H_2 has been shown to be effective in removing surface HCl [11] and the secondary reflux treatment serves to extract the "inbuilt" Cl component [28]. All the reaction data presented here were generated in the absence of any significant catalyst deactivation. Each catalytic run was repeated (up to six times) using different samples from the same batch of catalyst and the measured rates did not deviate by more than $\pm 7\%$.

3. Results and discussion

The Ni catalysts considered in this study are listed in table 1, which includes the Ni loading, BET surface areas and TEM-derived surface-weighted average Ni particle diameter (and the range of diameters). The Ni particle size distributions for representative catalysts are shown in figure 1. Taking the family of Ni/SiO_2

Table 1
Nickel loading, BET surface areas, surface-weighted average Ni particle sizes and size range associated with activated supported Ni catalysts prepared by impregnation and precipitation–deposition

Catalyst	Ni loading (% w/w)	N_2 BET surface area (m^2/g)	d_{Ni} (nm)	d_{Ni} range (nm)
Prepared by impregnation				
Ni/SiO_2	4.5	236	7.3	<1–15
Ni/SiO_2	8.9	203	9.4	<1–20
Ni/SiO_2 [a]	8.9	208	11.7	<1–25
Ni/Al_2O_3	8.4	120	5.3	<1–10
Ni/MgO	8.6	105	9.8	<1–20
Ni/AC	8.3	904	22.1	<5–80
Ni/graphite	9.8	10	25.0	<5–80
Prepared by precipitation–deposition				
Ni/SiO_2	1.5	240	1.4	<1–4
Ni/SiO_2	6.2	226	1.8	<1–5
Ni/SiO_2	10.5	223	2.3	<1–8
Ni/SiO_2 [a]	10.5	215	2.1	<1–8
Ni/SiO_2	15.2	216	3.1	<1–8
Ni/SiO_2	20.3	208	3.7	<1–10

[a] With precalcination.

catalysts, sample preparation by precipitation–deposition has been shown elsewhere to generate smaller average Ni particle diameters than the less controlled $Ni(NO_3)_2$ impregnation [27,29]. The former synthesis route involves the precipitation of an Ni(II) phase on to the silica support through the basification of a nickel salt solution–silica suspension via the decomposition of urea which, upon activation, generates a nickel phyllosilicate phase that is responsible for enhanced Ni dispersion [29]. In contrast, Ni/SiO_2 prepared by impregnation exhibits weaker interaction with the substrate and a greater tendency for Ni agglomeration and growth [27],

Table 2
Surface-weighted average Ni particle sizes based on H_2 chemisorption (d_H) and TEM (d_{TEM}) measurements

Catalyst	Ni (% w/w)	d_H (nm)	d_{TEM} (nm)
Ni/SiO_2 [a]	10.5	2.3	3.3
Ni/SiO_2	8.9	9.4	11.2
Ni/Al_2O_3	8.4	5.3	5.9
Ni/MgO	8.6	9.8	12.5
Ni/AC	8.3	22.1	21.4
Ni/graphite	9.8	25.0	27.2

[a] Prepared by precipitation–deposition.

resulting in larger Ni particles under the same activation conditions. At higher Ni loadings, the particles are in closer proximity and agglomeration is better facilitated with a resultant increase in size (table 1). Precalcination of the deposited Ni/SiO_2 had little effect on the ultimate Ni dimensions but the oxidative treatment of the impregnated precursor contributed to sintering and resulted in larger average Ni diameters, as has been noted elsewhere [30]. The average Ni particle diameters obtained from H_2 chemisorption (d_H) are compared in table 2 with those derived from TEM analysis (d_{TEM}). Although there is a mismatch in the Ni particle sizes derived from the two techniques (d_{TEM} typically lower than d_H), the overall sequence of increasing Ni diameter is the same in both cases. The discrepancy in particle size measurements can be attributed [31] to (i) limitations of the TEM analysis, where insufficient contrast in the image can hamper an accurate analysis, and/or deviation from an exclusive 2:1 H:Ni adsorption stoichiometry, as is normally applied in H_2 chemisorption analysis.

Representative low-resolution TEM images are included in figure 2 to illustrate the nature of the Ni

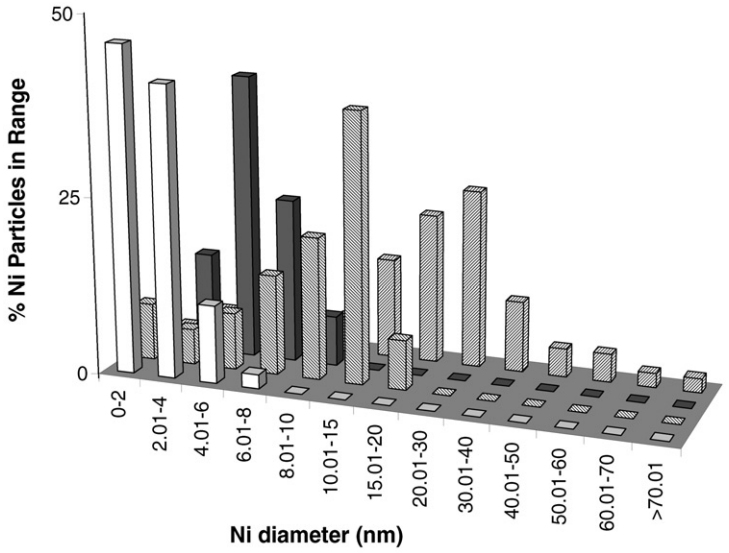

Figure 1. Nickel particle size distributions associated with freshly reduced (without precalcination) Ni/SiO_2 prepared by precipitation–deposition (10.5% w/w Ni, open bars) and impregnation (8.9% w/w Ni, downward hatched bars) and impregnated Ni/Al_2O_3 (solid bars), and Ni/AC (upward hatched bars).

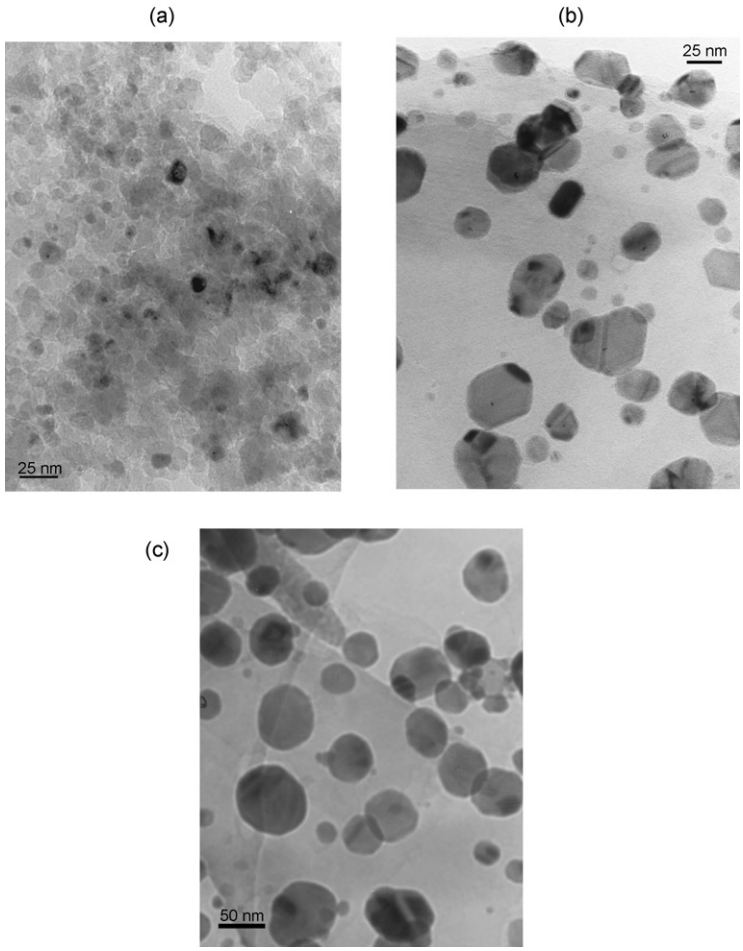

Figure 2. Representative low-resolution TEM images of (a) Ni/Al_2O_3, (b) Ni/graphite and (c) Ni/AC.

dispersion/morphology. The range of size distributions (figure 1 and table 1) and morphologies (figure 2) associated with the Ni phase dispersed on the different supports, at a comparable Ni loading, are inherent features of the interfacial energies associated with each system [32]. We have considered an array of substrates, ranging from a basic MgO to conventional Al_2O_3 and SiO_2, graphite which is known [33] to interact strongly with supported metals, and a high surface area activated carbon (AC) with little or no metal–support interaction. The latter can be assessed from the TEM images given in figure 2 where the Ni particles supported on AC exhibit an indistinct or globular geometry that has been shown to be diagnostic of limited metal–support interaction [34], while the metal phase associated with the graphite substrate shows evidence of faceting that reflects stronger surface interactions. Activation of Ni/MgO yielded a surface metal morphology similar to that associated with Ni/SiO_2 with a comparable size distribution. The Ni phase associated with Al_2O_3 is characterized by the narrowest distribution (figure 1) of smaller crystallites; the average Ni diameter was the lowest of the five supported systems. The latter finds support in earlier work reported by Hoang-Van *et al*. [35] and the suppression of particle growth has been attributed to the ionic nature of the $Ni–Al_2O_3$ interaction, leading to an enhanced dispersion of electron deficient Ni [36]. The Ni-impregnated activated carbon (AC) and graphite showed the widest range of sizes and highest average values. Reduction of Ni supported on AC, an amorphous substrate with a high BET surface area (table 1), involves significant concomitant Ni agglomeration due to the limited Ni–substrate interaction and inherent higher metal particle mobility. Graphite has a low BET surface area with few edge positions available for depositing the supported metal, which, as a direct consequence, is present in the form of larger particles at this loading.

In every case, the supported Ni catalysts served only to cleave the C–Cl bond in the presence of H_2 gas, leaving the aromatic nucleus intact, i.e., 100% HDC selectivity. The latter suggests that the dechlorinated product, once generated, desorbs from the surface whereas, in the activation step, the resonance energy of the aromatic ring is not significantly disrupted. Such reaction selectivity is significant in that Pd- and Rh-based catalysts (under comparable reaction conditions) have been reported [6,7] to convert chlorobenzene

Table 3
Potentiometric analysis of the Cl content of the used (impregnated) catalysts after thermal desorption (reversible) and extraction (irreversible): total CB reacted = 8.8×10^{-3} mol

Catalyst	Total Cl/Ni	"Reversibly" held Cl (%)	"Irreversibly held" Cl (%)
Ni/SiO_2	0.1	60	40
Ni/Al_2O_3	0.7	56	44
Ni/MgO	2.4	31	69
Ni/AC	<0.1	62	38
Ni/graphite	<0.1	65	35

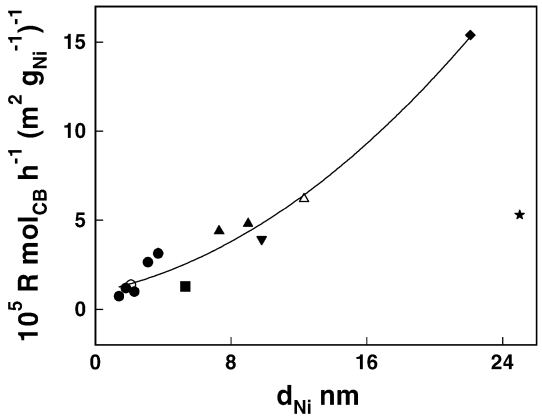

Figure 3. Specific CB HDC rate (R) as a function of the surface-weighted average Ni particle diameter (d_{Ni}) for reaction over impregnated Ni/SiO_2 (▲; with precalcination, △), Ni/Al_2O_3 (■), Ni/MgO (▼), Ni/AC (◆), Ni/graphite (★) and Ni/SiO_2 prepared by precipitation–deposition (●; with precalcination, ○).

further to cyclohexane, i.e., additional ring hydrogenation. Chlorine is cleaved from the aromatic host as HCl and there was no evidence of any Cl_2 formation. It was shown elsewhere [11] that the catalyst surface, under HDC reaction conditions, is saturated with HCl. Moreover, STEM/EDX elemental maps of used catalysts revealed an appreciable halogen concentration on the surface [37]. We determined the "reversibly" and "irreversibly" held halogen components on the used catalysts by a potentiometric methodology (see Experimental section). The co-existence of reversibly and irreversibly bound Cl on the catalyst surface during HDC has been established elsewhere [6,14]. We have shown previously [28] that, in the case of Ni/SiO_2, the irreversibly bound Cl is associated with the surface Ni sites. Potentiometric determination of our scrubbing solution (containing the reversibly held halogen) and refluxed water extract (containing the irreversibly held halogen) yielded the results provided in table 3. A subsequent elemental mapping of the refluxed solid did not reveal even trace quantities of halogen on the surface, i.e., the combined thermal desorption (in H_2) and reflux treatment were fully effective in extracting the entire halogen component from the spent catalysts. There was an appreciably higher residual Cl content (tabulated as a Cl/Ni molar ratio) associated with the used Ni/MgO and (to a lesser extent) Ni/Al_2O_3. Moreover, the Ni/MgO bore a higher component of strongly (irreversibly) held Cl that was only removed from the catalyst after heating under reflux. The other four catalysts exhibited a roughly equivalent reversible/irreversible halogen distribution. The basic character of the MgO substrate [38] distinguishes this support from the others and must be the source of the higher affinity for HCl attachment.

The specific HDC rate (per unit exposed nickel surface area) is plotted as a function of Ni particle size in figure 3. Under the reaction conditions employed in this study, there was no appreciable Ni growth (from TEM analysis) over the limited period of HDC. Moreover, the HDC consumption rates represent steady-state values with no evidence of any significant catalyst deactivation. The overall trend points to higher specific chlorine removal rates over larger Ni particles, an observation that falls in line with a consensus that is emerging from the literature of higher dehalogenation rates associated with lower metal dispersions [20–22]. The exception to this effect is Ni/graphite, which delivered a specific HDC rate that fell well below the common trend line. Reaction over Ni/Al_2O_3 also deviated somewhat from the trend, with a distinctly lower rate. It is known that the nature of the support can influence catalyst performance [39], where metal–support interactions can have significant catalytic implications [40]. We have adopted the notion of structure sensitivity in the broad sense where metal particle size effects can be linked to the metal ensemble size with the associated intrinsic electronic properties and any perturbation(s) due to metal–support interactions. Support-induced electronic effects are considered to be negligible for larger (ca. 10–40 nm) metallic particles [41]. The distribution of Ni particle size associated with these catalysts (table 1 and figure 1) is such that support effects can contribute, to varying extents, to the metal site activity. The lower specific activities associated with Ni/graphite (in particular) and Ni/Al_2O_3 may then be ascribed, at least in part, to electron transfer with the support medium that induces electronic perturbations in the dispersed Ni phase. The high surface area AC exhibits little or no metal–support interaction and the larger Ni particles exhibit the highest intrinsic HDC activity. Gas-phase hydrogenolysis reactions over supported metal systems are known to display a distinct structure sensitivity [42–44]. The data presented in figure 3 suggest that this extends to the hydrogenolytic cleavage of the C–Cl bond in CB. Stakheev and Kustov, in their comprehensive review of catalyst support effects [45], demonstrated the manner in which hydrogenolysis reactions are strongly influenced by the electronic structure of the active metal sites. Particle size, surface morphology and the preponderance of a particular exposed crystal plane can all impact on the ultimate level of dechlorination where the effect on

hydrogen chemisorption/activation has been suggested to influence hydrogenolysis activity significantly [42]. Indeed, in a previous study [26], we examined the H_2 TPD characteristics for Ni/SiO_2 and tentatively attributed different forms of surface hydrogen as participating in hydrogen addition and/or hydrogen scission reactions; the involvement of spillover hydrogen in HDC has been proposed [46]. Work is now under way to probe the nature of the surface hydrogen associated with the catalysts considered in this study as a means of accounting for the observed differences in intrinsic HDC activity. Moreover, the use of supported Ni systems where catalyst preparation/activation ensures that the majority of the Ni particles have diameters <5 nm will facilitate an implicit assessment of structure sensitivity.

4. Conclusions

Gas-phase HDC of chlorobenzene to benzene over supported Ni is structure sensitive, the specific HDC rate being enhanced over larger Ni particles that have limited support interaction. The Ni metal phase exhibited a morphological diversity and the average Ni size at a comparable metal loading ($9 \pm 1\%$ w/w) decreased (from 25.0 to 5.3) in the following sequence: Ni/graphite $\sim Ni/AC > Ni/MgO \sim Ni/SiO_2 > Ni/Al_2O_3$. Preparation of Ni/SiO_2 by precipitation–deposition delivered an appreciably narrower distribution of smaller Ni particles than the impregnation route. The used catalysts contain a significant chlorine component that is significantly greater and more strongly bound to the MgO-supported Ni catalyst.

Acknowledgments

We are grateful to Rik Brydson, George Tavoularis and Gonzalo Pina for assistance with the TEM analysis and catalysis measurements. M.A.K. acknowledges partial support for this work from the National Science Foundation through Grant CTS-0218591.

References

[1] J.K. Fawell and S. Hunt, *Environmental Toxicology, Organic Pollutants* (Ellis Horwood, Chichester, 1988).
[2] C. Denbesten, J.J.R.M. Vet, H.T. Besselink, G.S. Kiel, B.J.M. Vanberkel, R. Beems and P.J. Vandladeren, Toxicol. Appl. Pharm. 11 (1991) 69.
[3] J.F. McEldowney and S. McEldowney, *Environment and the Law* (Longman, Harlow, 1996).
[4] H. Hagenmaier, K. Horch, H. Fahlenkamp and G. Schetter, Chemosphere 23 (1991) 1429.
[5] M. Kraus and V. Bazant, in: *Proceedings of the 5th International Congress on Catalysis*, ed. J.W. Hightower (North-Holland, New York, 1973), p. 1073.
[6] B. Coq, G. Ferrat and F. Figueras, J. Catal. 101 (1986) 434.
[7] P. Bodnariuk, B. Coq, G. Ferrat and F. Figueras, J. Catal. 116 (1989) 459.
[8] R. Gopinath, K.N. Rao, P.S.S. Prasad, S.S. Madhavendra, S. Narayanan and G. Vivekanandan, J. Mol. Catal. A: Chem. 181 (2002) 215.
[9] E.J. Creyghton, M.H.W. Burgers, J.C. Jensen and H. van Bekkum, Appl. Catal. A: Gen. 128 (1995) 275.
[10] G. Tavoularis and M.A. Keane, J. Mol. Catal. A: Chem. 142 (1999) 187.
[11] G. Tavoularis and M.A. Keane, J. Chem. Technol. Biotechnol. 74 (1999) 60.
[12] G. Tavoularis and M.A. Keane, Appl. Catal A: Gen. 182 (1999) 309.
[13] B.F. Hagh and D.T. Allen, Chem. Eng. Sci. 45 (1990) 2695.
[14] J. Estellé, J., Ruz, Y. Cesteros, R., Fernandez, P., Salagre, F., Medina and J.-E. Sueiras, J. Chem. Soc., Faraday Trans. 92 (1996) 2811.
[15] A.R. Suzdorf, S.V. Morozov, N.N. Anshits, S.I. Tsiganova and A.G. Anshits, Catal. Lett. 29 (1994) 49.
[16] B.F. Hagh and D.T. Allen, AIChE J. 36 (1990) 773.
[17] J. Frimmel and M. Zdražil, J. Catal. 167 (1997) 286.
[18] D.I. Kim and D.T. Allen, Ind. Eng. Chem. Res. 36 (1997) 3019.
[19] N. Lingaiah, M.A. Uddin, A. Muto, T. Iwamoto, Y. Sakata and Y. Kasano, J. Mol Catal. A: Chem. 161 (2000) 157.
[20] W. Juszczyk, A. Mallinowski and Z. Karpinski, Appl. Catal. A: Gen. 166 (1998) 311.
[21] M.A. Armendia, V. Boráu, I.M. Garcia, J.M. Jiménez, J.M. Marinas and F.J. Urbano, Appl. Catal. B: Environmental 20 (1999) 101.
[22] M.A. Armendia, V. Boráu, I.M. Garcia, C. Jiménez, A. Marinas, J.M. Marinas and F.J. Urbano, J. Catal. 187 (1999) 392.
[23] L. Prati and M. Rossi, Appl. Catal. B: Environ. 23 (1999) 135.
[24] Z.C. Zhang and B.C. Beard, Appl. Catal. A 174 (1998) 33.
[25] A. Gampine and D.P. Eyman. J. Catal. 170 (1998) 315.
[26] E.-J. Shin, A. Spiller, G. Tavoularis and M.A. Keane, Phys. Chem. Chem. Phys. 1 (1999) 3173.
[27] M.A. Keane, Can. J. Chem. 72 (1994) 372.
[28] C. Park, C. Menini, J.L. Valverde and M.A. Keane, J. Catal. 211 (2002) 451.
[29] P. Burattin, M. Che and C. Louis, J. Phys. Chem. B 103 (1999) 6171.
[30] G.A. Martin, C. Mirodatos and H. Praliaud, Appl. Catal. 1 (1981) 367.
[31] N. Mahata, K.V. Raghavan, V. Vishwanathan, C. Park and M.A. Keane, Phys. Chem. Chem. Phys. 3 (2001) 2712.
[32] R.T.K. Baker, J. Catal. 63 (1980) 523.
[33] N.M. Rodriguez, J. Mater. Res. 8 (1993) 3233.
[34] R.T.K. Baker, E.B. Prestridge and R.L. Garten, J. Catal. 59 (1979) 293.
[35] C. Hoang-Van, Y. Kachaya and S.J. Teichner, Appl. Catal. 46 (1989) 281.
[36] M.I. Zaki, Stud. Surf. Sci. Catal. 100 (1996) 569.
[37] C. Menini, C. Park, R. Brydson and M.A. Keane, J. Phys. Chem. B 104 (2000) 4281.
[38] A. Stevenson, J.A. Dumesic, R.T.K. Baker and E. Ruckenstein, *Metal Support Interactions in Catalysis, Sintering and Redispersions* (Van Nostrand Reinhold, New York, 1989).
[39] V. Ponec, Stud. Surf. Sci. Catal. 11 (1982) 63.
[40] G.C. Bond, Chem. Soc. Rev. 20 (1991) 441.
[41] M.C.J. Bradford and M.A. Vannice, Appl. Catal. A: Gen. 142 (1996) 73.
[42] G.C. Bond and J.C. Slaa, J. Chem. Technol. Biotechnol. 65 (1996) 15.
[43] M. Che and C.O. Bennett, Adv. Catal. 36 (1989) 55.
[44] B. Coq, A. Bittar and F. Figueras, J. Mol. Catal. 55 (1989) 34.
[45] A.Y. Stakheev and L.M. Kustov, Appl. Catal. A: Gen. 188 (1999) 3.
[46] G. Tavoularis and M.A. Keane, React. Kinet. Catal. Lett. 78 (2003) 11.